A Linear Material Model for Fiber-Induced Anisotropy of the Anulus Fibrosus

Dawn M. Elliott

Lori A. Setton

Department of Biomedical Engineering,
Duke University,
Durham, NC 27708

The anulus fibrosus (AF) is a lamellar, fibrocartilaginous component of the intervertebral disc, which exhibits highly anisotropic behaviors in tension. These behaviors arise from the material's unique collagen structure. We have investigated the use of a linear, fiber-induced anisotropic model for the AF using a quadratic strain energy density formulation with an explicit representation of the collagen fiber populations. We have proposed a representative set of intrinsic material properties using independent datasets of the AF from the literature and appropriate thermodynamic constraints. The model was validated by comparing predictions with previous experimental data for AF behavior and its dependence on fiber angle. The model predicts that compressible effects may exist for the AF, and suggests that physical effects of the equivalent ''matrix,'' ''fiber,'' ''fiber–matrix,'' and ''fiber–fiber,'' interactions may be important contributors to the mechanical behavior of the AF. [S0148-0731(00)00802-5]

Introduction

The intervertebral disc is a cartilaginous structure that functions to distribute loads and to provide for motion and flexibility of the spine [1]. Changes in disc composition, structure, and mechanics with aging, degeneration, and injury are considered to play important roles in low back pain [2]. The anulus fibrosus (AF) is a lamellar, fibrocartilaginous structure on the periphery of the intervertebral disc, which is an important contributor to the disc's mechanical function. The AF is composed principally of water (60–70 percent), collagen (50–70 percent by dry weight), aggregating and nonaggregating proteoglycans (10–20 percent by dry weight), and noncollagenous proteins (~25 percent by dry weight) [3]. The AF structure is highly organized into distinct lamellae [4] containing large collagen fiber bundles oriented at 28–43 deg to the transverse plane of the spine [5–7]. Studies have shown that more than half of the lamellae terminate or originate within any 20 deg span of the AF [4]. Successive lamellae have collagen fibers oriented at angles alternating above and below the plane (see Fig. 1). The highly organized structure of the AF produces material behavior that is anisotropic, principally in tension, with orders of magnitude differences in the tensile stiffness for samples oriented in the circumferential [8–11], axial [12,13], and radial directions [14,15]. The structural organization of collagen strongly influences the tensile behavior observed in the AF because collagen is the primary component responsible for withstanding tensile loads in fibrillar soft tissues such as the AF. The AF is significantly loaded in tension during physiological joint motions due to interstitial swelling effects as well as applied joint loads, which give rise to anulus bulging and deformation [16,17]. Anisotropic effects arising from the material's unique collagen structure may therefore be very important in providing for stiffness in the disc sufficient to support the large loads of daily activity.

The highly oriented structure of the AF suggests the utility of a material model with explicit representation of the collagen fibers and their mechanical contribution to disc function. Several investigators have developed finite element models for the spine motion segment, describing the AF as a fiber-reinforced composite. In these models, the collagen fibers of the AF have been represented by tension-only ''cable'' elements embedded within an isotropic ground substance (e.g., [18–22]). Such models have been applied to predict the magnitude of stresses and strains in the AF and motion segment under various physiological loads, such as axial compression, torsion, flexion–extension, or combined loading. Predictions of these models have suggested that AF strains are nonuniform and tensile in the circumferential direction, with values that are generally less than 0.10 in the nondegenerate disc under physiological loading [20,21]. Simulated disc degeneration has been used to study the mechanisms for initiation of tears, fissures, and cracks in the AF. These models have suggested potential mechanisms for AF failure including elevated interlaminar shear stresses in the posterior AF [19], elevated radial stresses and strains following depressurization of the nucleus pulposus [20,21], and propagation of discrete annular tears [23]. A significant limitation of predictions made previously with these models is their dependence upon material property datasets that were incomplete and lacking in material validation. In some studies, values for the material properties of the AF were determined by optimization of model predictions to experimentally measured structural parameters such as compressive displacement of the disc, radial ''bulge,'' end plate deformation, or intradiscal pressure [18–22]. Alternatively, material properties have been determined from estimated properties of isolated collagen fiber and isotropic ground substance, properties that have not been explicitly measured for this material [19–21]. Additionally, the dependence of model predictions on parameters such as fiber density, fiber-matrix interactions, and lamellar geometry, which may not be presently attainable, further limit the utility of this approach to fiber-reinforced modeling of the AF. In motion segment modeling, alternatives to representing the AF as a fiber-reinforced composite include representing the AF as an orthotropic continuum [23–25]. The predictions of these models for AF behavior are generally consistent with the fiber-reinforced models, although these predictions are again dependent upon inadequate and poorly validated material property datasets. More recent advances in modeling of the intervertebral disc have included the porous and permeable nature of the AF by modeling the material as a poroelastic medium [26–29]. The predictions of multiphasic models depend heavily upon material properties governing dilatational behaviors for the AF in tension (e.g., Poisson's ratio, bulk modulus, hydraulic permeability), few of which are available for anisotropic fiber-reinforced materials such as the AF.

An alternative approach to motion segment modeling was pro-

Contributed by the Bioengineering Division for publication in the JOURNAL OF BIOMECHANICAL ENGINEERING. Manuscript received by the Bioengineering Division September 13, 1999; revised manuscript received October 18, 1999. Associate Technical Editor: L. J. Soslowsky.

posed by Wu and Yao [11], to use a continuum material model for the solid matrix of the AF incorporating the effect of the oriented collagen matrix. A hyperelastic material model was proposed with an explicit dependence on invariants of the Eulerian strain tensor and vectors describing the collagen fiber populations, as outlined by Spencer [30,31]. Material property determinations were based on matching model predictions to independent material tests of the AF in tension, which demonstrated nonlinear and anisotropic behaviors. The properties obtained in their study, however, were restricted to states of pure stretch, thus limiting the applicability of their formulation for describing other deformation states. In addition, a constraining assumption was made in their model of incompressible behavior for the AF, which allowed the investigators to reduce the number of independent invariants and material coefficients. Volumetric changes due to fluid exudation and interstitial fluid redistribution within the tissue are believed to be important features of AF mechanics [1,29,32], however, so that a material model for the solid matrix of the AF as a compressible material may be essential for models describing both solid matrix behaviors and multiphasic interactions in the intervertebral disc.

The purpose of this study is to apply an anisotropic model, with an explicit representation of collagen fiber orientation and allowing for compressible material behavior, to describe the fiber-induced anisotropy of the solid matrix of the anulus fibrosus. A linear formulation is proposed based on a complete set of invariants incorporating the material and geometric parameters of the matrix and fibers. A representative set of material coefficients for the model is determined from independent, uniaxial material tests of the AF available in the literature and thermodynamic constraints. Model validation is achieved by comparison of the model predictions with previously reported measures of the dependence of AF tensile behavior on fiber angle (i.e., for the radial position at the outer and inner AF) and for the tensile properties of a single lamella of AF. This model is used to evaluate the significance of compressible effects in the AF as well as the physical contributions of equivalent ''matrix,'' ''fiber,'' ''fiber–matrix,'' and ''fiber–fiber'' interactions represented by the anisotropic formulation. The results of the development and validation for this linear formulation may serve as the foundation for the development of a nonlinear hyperelastic formulation that is physically appropriate and has reduced mathematical complexity.

Material Description

The AF was modeled as a continuum containing two populations of fibers assumed to be of equal density and uniform distribution within an isotropic matrix, as originally described by Spencer [30,31]. An orthonormal coordinate system is defined at a point in the AF such that $\mathbf{x}_1$ denotes the circumferential direction, $\mathbf{x}_2$ the axial direction, and $\mathbf{x}_3$ the radial direction of the disc (Fig. 1). Fiber orientations are denoted by unit vectors **a** and **b**, as shown in Fig. 2. The fiber vectors are assumed to be coplanar and separated by the angle 2ϕ. To allow a general representation of the fiber populations to a global coordinate system, the bisector to the fiber populations is defined at an angle θ to the $\mathbf{x}_1$ axis. Unit vectors for the fiber direction are $\mathbf{a}=(\cos(\theta-\phi),\sin(\theta-\phi),0)$ and $\mathbf{b}=(\cos(\theta+\phi),\sin(\theta+\phi),0)$. This representation of fiber populations using two angles (ϕ and θ) allows for independent consideration of the effect on the material behaviors of changes in the angle between the fibers (2ϕ) and of rotations of the fibers with respect to the global coordinate system (θ). When comparing model predictions to material property measures for the AF, θ will most often be taken to be zero. A physical representation of the fiber orientation is desired that is independent of the sign for **a** or **b**, so that symmetric structural tensors **A** and **B** are constructed from the dyads $\mathbf{A}=\mathbf{aa}$ and $\mathbf{B}=\mathbf{bb}$.

In the linear formulation, a strain energy density (W) may be defined for an isotropic material with two populations of fibers from the integrity basis of invariants of the infinitesimal strain tensor (ε) and the two structural tensors, **A** and **B** [33]. The strain energy is required to be symmetric with respect to the structural tensors, and a second-order function of the infinitesimal strain tensor as,

$$W=m_1I_1^2+m_2I_2+m_3I_1I_3+m_4I_3^2+m_5I_4+m_6I_5^2+m_7I_1I_5+m_8I_3I_5+m_9I_6, \tag{1}$$

where

$$\begin{aligned} I_1&=\operatorname{tr}\varepsilon & I_4&=\operatorname{tr}\mathbf{A}\varepsilon^2+\operatorname{tr}\mathbf{B}\varepsilon^2\\ I_2&=\operatorname{tr}\varepsilon^2 & I_5&=\operatorname{tr}\mathbf{AB}\varepsilon+\operatorname{tr}\mathbf{BA}\varepsilon\\ I_3&=\operatorname{tr}\mathbf{A}\varepsilon+\operatorname{tr}\mathbf{B}\varepsilon & I_6&=(\operatorname{tr}\mathbf{A}\varepsilon)(\operatorname{tr}\mathbf{B}\varepsilon). \end{aligned} \tag{2}$$

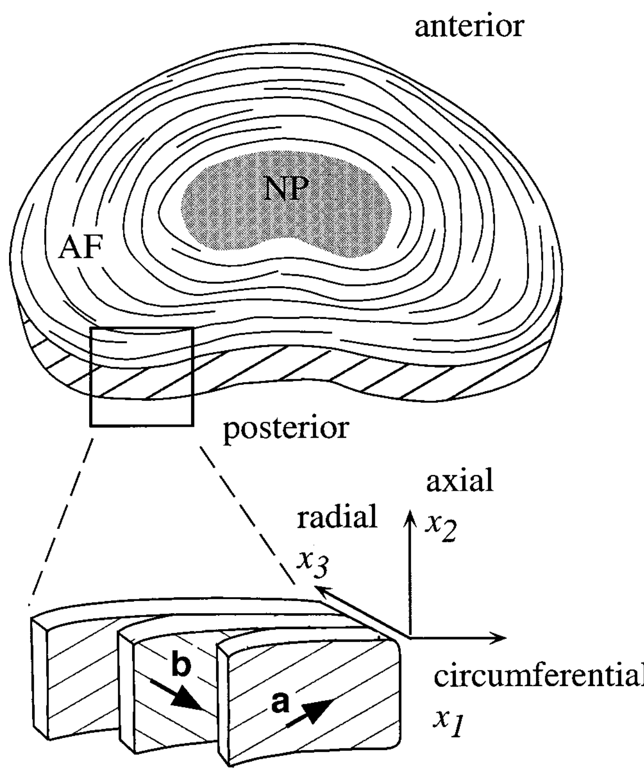

Fig. 1 Schematic of the intervertebral disc. Collagen fiber angles change with alternating lamellae in the anulus fibrosus. AF=anulus fibrosus, NP=nucleus pulposus. Unit vectors a and b denote orientation of collagen fiber populations in the x_1-x_2 plane.

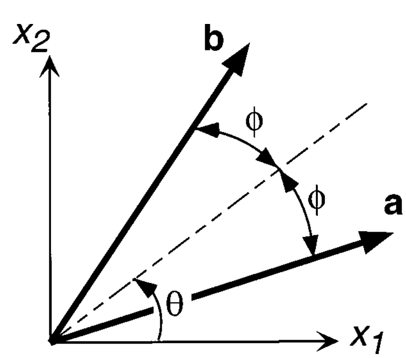

Fig. 2 Coordinate system used in model development. Unit vectors a and b denote orientation of collagen fiber populations in the x_1-x_2 plane. The fiber populations are oriented at an angle θ from the global coordinate system and at an angle 2ϕ from each other.

Note that the first two invariants are consistent with representations for an isotropic material. The remainder of the invariants represent mechanical contributions from fiber strains, and interactions of the fibers with the matrix or with each other. The material exhibits orthotropic symmetry, which is consistent with a set of nine independent material coefficients, m_1-m_9. For linear theory, these material properties are functionally related to the independent components of the elasticity tensor as [34],

$$\sigma=\partial W/\partial \varepsilon=\mathbf{C}\varepsilon, \tag{3}$$

where σ is the stress tensor and $\mathbf{C}$ is the fourth-order elasticity tensor (see appendix). Engineering constants describing uniaxial stress–strain relations (e.g., E_i, G_{ij}, and ν_{ij}) may be readily obtained from the components of $\mathbf{C}$, and therefore from the material coefficients, m_1-m_9. An advantage to use of the material coefficients m_1-m_9 is that they are invariant under changes in fiber angle, as fiber angle is an explicit variable in the strain energy formulation. Many of these engineering constants have been directly measured for the AF in independent, uniaxial material testing, and will be used for determination of a representative material property dataset (m_1-m_9), as described below.

Material Property Determination

A representative set of material properties m_1-m_9 was determined for the AF from experimental data for the mechanical behavior of the AF available in the literature, with several additional model assumptions. Unless otherwise specified, experimental data are specific for AF taken from human, nondegenerate intervertebral discs from anterior outer sites. The engineering constants were evaluated from the material behavior in uniaxial testing at equilibrium or from quasi-static testing, and for small strain magnitudes only. The anterior outer site of the AF was selected to maintain a consistent fiber angle and uniform fiber density for material property determinations, since the fiber angle, fiber density, and collagen content and type may vary spatially within the disc [3–5]. For material property determination, the fiber angles as represented in Fig. 2 were taken as $\phi=30$ deg and $\theta=0$ deg, which correspond to the fiber angle in the anterior outer AF.

First, six independent datasets for the AF were analyzed to determine the uniaxial moduli in tension and shear, as shown in Table 1. Note that two engineering constants, the shear moduli, G_{13} and G_{23}, were assumed to be equal for insufficient evidence of large differences in the limited available data [35,36]. Second, the in-plane shear modulus, G_{12}, had not been previously measured; the assumption was made that G_{12} was equivalent to the two engineering constants, G_{13} and G_{23}, which describe out-of-plane shear moduli. Finally, the two remaining engineering constants, ν_{31} and ν_{32}, were constrained by the thermodynamic restrictions for positive definiteness of the elasticity tensor as,

$$\nu_{32}^2\frac{E_2}{E_3}+\nu_{31}^2\frac{E_1}{E_3}+\nu_{32}\nu_{31}\frac{2E_2\nu_{12}}{E_3}+\frac{\nu_{12}^2E_2-E_1}{E_1}\geqslant 0. \tag{4}$$

Using the values for the measured engineering constants in Table 1, a quadratic relationship between ν_{31} and ν_{32} was established. The maximum value for ν_{32} is 0.130, corresponding to $\nu_{31}=0$, and the maximum ν_{31} is 0.062, corresponding to $\nu_{32}=0$. Values for the material properties were found to be unbounded near these limits for ν_{31} and ν_{32}; therefore, approximate median values for ν_{31} and ν_{32} were taken as 0.020 and 0.065, respectively. The associated representative set of material properties, m_1-m_9, respectively, is therefore, 0.118, 0.100, 3.44, 25.0, 0.0, 17.3, −1.45, −20.1, and 0.0 MPa. This set of selected properties is thermodynamically permissible but not unique.

Table 1 Engineering constants for human anulus fibrosus from experimental testing[a]

Property	Source	Mean (SD)	Comments	Value chosen for model
E_1	[8]	27.1 (14.6)	*b*	35 MPa
	[9]	49.4 (32.7)	*c*	
	[11]	17.2	*d*	
E_2	[13]	8 (6)	*e*	8 MPa
E_3	[14]	0.19 (0.21)	*f*	0.2 MPa
ν_{12}	[8]	1.16 (0.68)	*g*	1.2
G_{13}	[35]	0.06 (0.02)	*h*	0.1 MPa
	[36]	0.105 (0.05)	*i*	
G_{23}	[35]	0.11 (0.03)	*h*	0.1 MPa

[a]Data presented for nondegenerate human AF from anterior outer sites, unless specified.
[b]Calculated at 75 percent of failure strain where failure strain was ~0.18.
[c]Calculated at 75 percent of failure strain where failure strain was ~0.1.
[d]Calculated from authors' figure as tangent to σ–λ curve at $\lambda=1.15$.
[e]2–3 year old ewes; calculated at 75 percent of failure strain where failure strain was ~0.18.
[f]Toe region modulus was used.
[g]Average value in the range 65–85 percent of failure strain, where failure strain was ~0.18.
[h]Data for 0 percent compressive clamping strain.
[i]Data for 0.02 shear strain.

Model Validation

Two methods were used for independent model validation. First, model predictions for the AF with variations in collagen fiber angle were compared to available data from independent experiments for the tensile behavior of the AF at the known fiber angles of 28 deg at the outer AF and 43 deg at the inner AF [5,8,9]. Second, the model was reduced to the case for a single lamella by setting the fiber angle, ϕ, to zero (i.e., a single population of fibers). Model predictions for the single lamella were then compared to available data from independent experiments for the tensile behavior of a single lamella in uniaxial testing [37].

Model predictions for the uniaxial modulus in the circumferential direction (E_1) are plotted in Fig. 3 as a function of fiber angle, ϕ. The predictions for the uniaxial tensile modulus in the circumferential direction can be compared to experimentally measured values at the outer AF (28 deg) and at the inner AF (43 deg) for anterior sites as shown [8,9]. The measured decrease in E_1 at the outer compared to the inner AF is consistent with model predictions based on the dependence on fiber angle alone. For $\phi=60$ deg, the model predicts a modulus $E_1=8$ MPa, which, as expected, is equivalent to E_2 at $\phi=30$ deg (Figs. 4(*a*, *b*)). For $\phi=90$ deg (Fig. 4(*c*)), there is no component of the fiber in the $\mathbf{x}_1$ direction ($E_1=0.28$ MPa) and the predicted modulus is equal to that in the radial direction (E_3, out of the fiber plane). In addition, the model predicts less than a 0.2 percent variation in the radial modulus (E_3) between the physiological fiber angle range of 28 to 43 deg, which is in agreement with the experimental finding of no significant changes in E_3 with position in the disc [14].

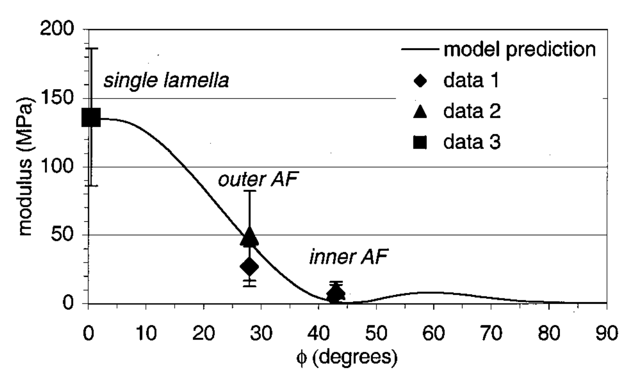

Fig. 3 Model prediction for modulus in the $\mathbf{x}_1$ direction for changing fiber angle, ϕ. Data 1 from [8], data 2 from [9], and data 3 from [37].

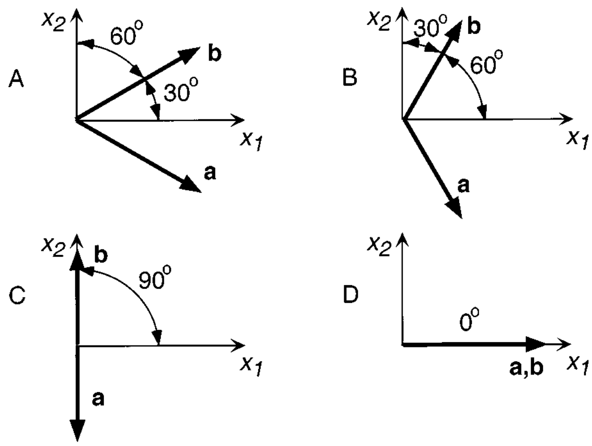

Fig. 4 Schematic of fiber populations for several orientations of fiber populations: (*A*) Physiologic representation of AF fiber populations was used to determine the material property set, $\theta=0$ deg and $\phi=30$ deg. (*B*) Fiber angle $\phi=60$ deg for $\theta=0$ deg; alternatively, may represent a coordinate rotation to $\theta=90$ deg while maintaining a physiologic angle $\phi=30$ deg. (*C*) For $\phi=90$ deg, the fiber populations coincide and represent the case of transverse isotropy, with the material properties in the x_1 direction being transverse to the fiber populations. (*D*) For $\phi=0$ deg, the fiber populations coincide and represent transverse isotropy, with the material properties in x_1 direction being in the fiber direction.

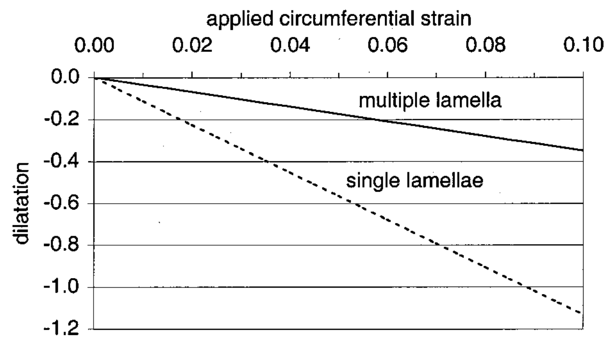

Fig. 5 Model prediction for dilatation for a multiple lamella AF at $\phi=30$ deg under uniaxial strain in the x_1 direction (circumferential) and for a single lamella under uniaxial strain in the fiber direction

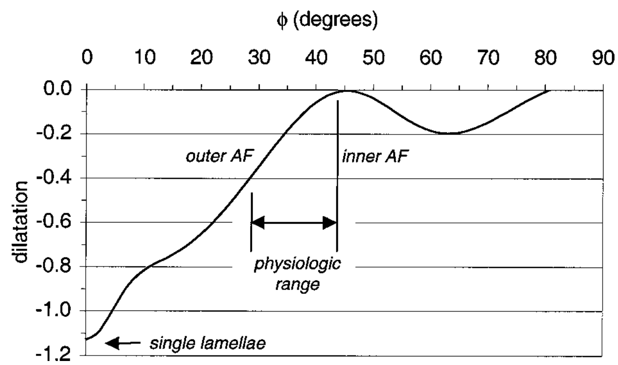

Fig. 6 Model prediction for dilatation for a uniaxial strain of 0.1 in the x_1 direction as a function of fiber angle, ϕ

By setting the fiber angle, ϕ, to zero, a model for transverse isotropy is obtained. For one fiber population, the full basis of invariants is:

$$J_1=\operatorname{tr}\varepsilon \qquad J_3=\operatorname{tr}\mathbf{A}\varepsilon$$

$$J_2=\operatorname{tr}\varepsilon^2 \qquad J_4=\operatorname{tr}\mathbf{A}\varepsilon^2. \tag{5}$$

Maintaining a strain energy formulation that is second-order in strain,

$$W=k_1J_1^2+k_2J_2+k_3J_1J_3+k_4J_3^2+k_5J_4, \tag{6}$$

we obtain a set of five material constants that are required to describe this material behavior. An explicit relationship was obtained between this reduced set of properties k_i, $i=1,5$ and the material properties for orthotropic symmetry, m_i, $i=1,9$. For the representative set of properties given in the previous section, a uniaxial modulus of 133.6 MPa was predicted for a single lamella tested in tension along the fiber direction. This value agrees extremely well with values of 136 ± 50 MPa for the uniaxial tensile modulus of single AF lamellae measured in independent testing [37], Fig. 3.

Model Predictions

A major objective in developing a fiber-induced anisotropic model for the AF is to examine the assumption of compressible behavior in the linear region. Model predictions for dilatation (i.e., I_1) within the linear region for a uniaxial tensile strain in the circumferential direction (Fig. 5) were determined using the representative set of material properties. The model predictions for a single lamella under uniaxial elongation in the fiber direction are also presented in Fig. 5. The predicted dilatation is negative for both single and multiple lamellae AF, with magnitudes that are approximately three times greater for the single lamella as compared to the multiple lamellae samples. This observation suggests that two fiber populations alternating at an angle of 30 deg will function to partly conserve volume while providing for considerable stiffness and strength. Variations in the predicted dilatation with changing fiber angle (ϕ) for the multiple lamellae geometry are shown in Fig. 6 at a fixed value of uniaxial tensile strain ($\varepsilon_{11}=0.1$). The predicted magnitude of the dilatation decreases for changes in fiber angle from outer to inner AF for a uniaxial stretch in the $\mathbf{x}_1$ direction.

Discussion

An anisotropic continuum model, which includes an explicit representation of the collagen fiber populations and their contribution to the mechanical behavior of the material, was applied to the solid matrix of the anulus fibrosus. A complete representative set of thermodynamically permissible material properties was obtained from independent, uniaxial tensile and shear material tests available in the literature, for specific physical assumptions and for appropriate thermodynamic restrictions. Model predictions for the mechanical behavior of the AF and its dependence on the angle between the fiber populations were compared to independent experimental data with favorable results. Very good agreement was also found for model predictions of the uniaxial tensile behavior of a single lamella compared to independent experimental data. These findings provide independent validation of the model and suggest its potential utility for studies of AF mechanics subjected to more complex loading configurations. Of interest was the prediction of a large, negative dilatation for the AF in response to a uniaxial tensile stretch. The predicted dilatation was larger for a single lamella containing one fiber population as compared to that predicted for two fiber populations. This result suggests that the existence of multiple layers of collagen fibers with alternating fiber orientations may function to provide tensile stiffness and strength in the AF while minimizing volumetric changes during loading.

The model utilized in this study was originally developed by Spencer for describing fiber-induced anisotropy in materials using an explicit dependence of the strain energy on invariants of the strain and structural tensors [30,31]. A similar approach was used by Wu and Yao [11] to model the AF using a nonlinear strain energy formulation and an assumption of material incompressibility. Their model development and material property determinations were limited by the assumption of material incompressibility and the available data, thus losing the generality of this model, including its ability to predict the more recent experimental data independently [8,14,35,36]. Investigators have also used fiber-reinforced continuum models to describe transverse-isotropy in other biological tissues including the ventricular myocardium and visceral pleura (e.g., [38–42]) and more recently ligaments [43]. In these studies, the basis of invariants was reduced by the assumption of incompressible behavior. This is a common and well-justified approach for tissues in which fluid exudation and redistribution (i.e., volumetric changes) may not be important contributors to the tissues' mechanical function. We have shown that volumetric loss may be an important feature of AF deformation, which is likely due to fluid exudation. Therefore, approaches that seek to reduce the integrity basis of invariants by making use of the incompressibility assumption may not be well justified for studies of the AF.

A major goal in applying this linear formulation to the AF was to assess the dominant terms that contribute to the constitutive law, toward the objective of obtaining a reduced set of invariants that can be used for future modeling of more mathematically complex, nonlinear behaviors. Toward this goal, all terms were retained in the strain energy density formulation, including those representative of ''matrix,'' ''fiber,'' ''matrix–fiber,'' and ''fiber–fiber'' interactions. This formulation gives rise to a set of nine independent and intrinsic material coefficients denoted by $m_1 - m_9$. We found that this set may be readily reduced by several relevant physical assumptions. The assumption of equivalent shear behaviors for the AF in-plane (G_{12}) and out-of-plane ($G_{13} = G_{23}$) allows for the elimination of the dependence on the invariants I_4 and I_6, and of material properties m_5 and m_9, reducing the material constants to a set of seven. This assumption is equivalent to neglecting mechanical contributions of the fibers to the shear stiffness of the material. While preliminary parametric studies support this physical assumption, more complete experimental studies of the AF in shear will be required to fully test its validity.

Of the remaining material properties, m_1 and m_2 represent contributions of the ''matrix'' and are analogous to the Lamé coefficients for an isotropic material. For values of m_1 and m_2 determined in this study (0.118 and 0.1 MPa, respectively), associated values for the Lamé coefficients may be obtained of $\lambda = 0.24$ MPa and $\mu = 0.10$ MPa. A uniaxial modulus for the AF may thus be obtained from $H_A = \lambda + 2\mu$ of 0.44 MPa, which agrees very well with values measured for the AF of $H_A = 0.25 - 0.45$ MPa in confined compression testing [32]. The material property m_4 represents in-plane mechanical contributions arising from stretch in the fiber direction. The large magnitude of m_4 suggests that stiffness along the fiber direction is a major contributor to its material behavior in tension.

The remaining terms in the strain energy formulation presented here may be considered to represent ''fiber–matrix'' interactions (i.e., denoted by coefficients m_3 and m_7) and ''fiber–fiber'' interactions (i.e., coefficients m_6 and m_8) in the AF. Nonzero values for the independent properties m_3 and m_7 indicate that an in-plane fiber stretch will give rise to ''bulk'' effects including dilatation and out-of-plane stresses and strains. In some previous models of transverse-isotropy of biological tissues, the mechanical contributions of these interactions have been neglected in order to reduce model complexity [38–43]. Our findings of a nonzero m_3 and m_7 suggests that fiber–matrix interactions may be important contributors to the stresses and strains within the AF. This is also apparent in a strong dependence of calculated values for the Poisson's ratios (ν_{31}, ν_{32}) on the material coefficient, m_3, demonstrating that fiber stretch is associated with bulk effects that may affect the in-plane, as well as out-of-plane stress–strain fields. This physical interpretation may be reasonable for collagenous tissues such as the AF, in which the large collagen fibers may have significant physical interactions with other matrix constituents such as the minor collagens (e.g., types III, V, VI, IX, XI), noncollagenous proteins and proteoglycans [3].

In this formulation, terms that represent mechanical contributions of ''fiber–fiber'' interactions (i.e., coefficients m_6 and m_8) were included. The presence of these terms, along with m_7, is the major difference between this model of orthotropic symmetry and that proposed by Spilker and co-workers [25] to describe the AF as alternating layers of a transversely isotropic material. In the AF, there exists potential for mechanical interactions between fibers and matrix in adjacent lamellae by mechanisms such as physical interactions between the minor collagens, noncollagenous proteins, and proteoglycans as described above. The physical mechanisms for interactions between the fibers in adjacent lamella is less intuitive, however, as the two fiber populations are physically isolated in the AF rather than uniformly distributed as proposed for this model formulation. In the model, ''fiber–fiber'' interactions, represented by the terms associated with m_6 and m_8, were found to be nonzero and large, suggesting that terms representing these interactions may be required to predict AF behaviors. This observation may point toward the physical significance of interlamellar interactions between adjacent lamella and at the origination and termination of layers throughout the tissue. Delamination or tears that have been observed to occur with intervertebral disc degeneration [2] may be related to these fiber–fiber interactions. Their relative importance in AF degeneration can be assessed by independent determinations of the intrinsic material coefficients for degenerated AF material using the approach outlined in this study.

The model proposed here is limited to study of loading configurations that place the collagen fibers into tension. Swelling mechanisms in the intervertebral disc may generate tensile strain in the material that are sufficient to ensure that the collagen fibers of the AF are primarily loaded in tension during functional loading of the spine [20,28]. In the absence of tensile strain within the collagen matrix, however, the large stiffness of the collagen fiber may not directly contribute to load support, as was apparent from our findings for similar uniaxial moduli for the ''matrix'' material in tension and compression. Indeed, the highly anisotropic behavior observed for the AF in tension is not exhibited in compressive loading of the material *in vitro* [44,45], although there is evidence in direct permeation tests that the hydraulic permeability exhibits minor anisotropy [46]. These results suggest that the orientation of the collagen fibers contributes little to the compressive behavior so that the material property determination and model validation using material behavior in tension as performed in this study may be appropriate.

In this study, we have limited our attention to descriptions of AF behavior under conditions of small strain. For larger strains, this model is limited both by our use of the infinitesimal strain tensor and by our assumption of a constant fiber angle under deformation. While *in situ* assessments of matrix strain, as well as FEM predictions, suggest that many physiological loads generate only small strains in the AF, the material behavior *in vitro* is clearly nonlinear [10]. Studies of the nonlinear behavior of the AF may be of particular importance in describing the behavior of the inner AF, adjacent to the nucleus pulposus, where larger deformations have been observed experimentally [47]. The approach outlined in our study may be modified to model nonlinear anisotropic phenomena in the AF by incorporating a strain tensor appropriate for finite deformations (e.g., Lagrangian or Eulerian) and by proposing a strain energy formulation with a nonlinear dependence on a prescribed set of invariants. The ability to work with a reduced set of invariants is particularly desirable in models of nonlinear behavior, due to the mathematical complexities associated with developing a nonlinear hyperelastic formulation. Importantly, our model for linear behavior and the associated material property determinations suggest that a reduced set of invariants may be useful and appropriate for describing the AF in tension.

In summary, we have applied and validated a linear anisotropic model to the anulus fibrosus, with an explicit representation of the collagen fiber populations in the material. The predictive ability of this model provides support for the utility of using structural tensors and a strain energy formulation for modeling fiber-induced anisotropy in cartilaginous tissues. We have proposed a set of intrinsic material properties based upon experimental data available in the literature. We have suggested a mechanical contribution for the equivalent ''fiber'' and ''matrix'' components of the AF microstructure that may guide the selection of a nonlinear, hyperelastic model formulation. Future work will focus on using this material description of fiber-induced anisotropy for the AF as the solid phase of a multiphasic material, examining anterior to posterior spatial variation, and evaluating the effect of disc degeneration.

Acknowledgments

This work was supported by research grants from the NSF (Grant No. BES-9703299) and a predoctoral training grant from the NIH.

Appendix

The functional relationship between the components of the elasticity tensor (**C**) and the material coefficients (m_1–m_9) of the strain energy density function (W) in Eq. (1) are developed by evaluating Eq. (3). Given below are the resulting functions for the coordinate system defined in Fig. 2 and for $\theta=0$.

$$c_{1111}=2(m_1+m_2)+(1+\cos 2\phi)(2m_3+2m_5+2m_7\cos 2\phi) + (1+\cos 2\phi)^2(2m_4+2m_6\cos^2 2\phi+2m_8\cos 2\phi+\tfrac{1}{2}m_9)$$

$$c_{2222}=2(m_1+m_2)+(1+\cos 2\phi)(2m_3+2m_5-2m_7\cos 2\phi) + (1-\cos 2\phi)^2(2m_4+2m_6\cos^2 2\phi-2m_8\cos 2\phi+\tfrac{1}{2}m_9)$$

$$c_{3333}=2(m_1+m_2)$$

$$c_{2323}=m_2+\tfrac{1}{2}m_5(1-\cos 2\phi)$$

$$c_{2131}=m_2+\tfrac{1}{2}m_5(1+\cos 2\phi)$$

$$c_{1212}=m_2+m_5-\tfrac{1}{2}m_9(1-\cos^2 2\phi)$$

$$c_{1122}=2(m_1+m_3)+2m_7\cos^2 2\phi+(1-\cos^2 2\phi) \times(2m_4-2m_6\cos^2 2\phi+\tfrac{1}{2}m_9)$$

$$c_{1133}=2m_1+(1+\cos 2\phi)(m_3+m_7\cos 2\phi)$$

$$c_{2233}=2m_1+(1-\cos 2\phi)(m_3-m_7\cos 2\phi)$$

References

[1] Weidenbaum, M., Iatridis, J., Setton, L. A., Foster, R. J., and Mow, V. C., 1996, ''Mechanical Behavior of the Intervertebral Disc and the Effects of Degeneration,'' in: *Low Back Pain: A Scientific and Clinical Overview*, J. N. Weinstein and S. L. Gordon, eds., American Academy of Orthopaedic Surgeons, pp. 557–582.

[2] Goel, V. K., 1996, ''Biomechanics of Disc Herniation and Related Issues,'' in: *Low Back Pain: A Scientific and Clinical Overview*, J. N. Weinstein and S. L. Gordon, eds., American Academy of Orthopaedic Surgeons, pp. 289–304.

[3] Bayliss, M. T., and Johnstone, B., 1992, ''Biochemistry of the Intervertebral Disc,'' in: *The Lumbar Spine and Back Pain*, M. I. V. Jayson and A. S. J. Dixon, eds., Churchill Liningstone, pp. 111–131.

[4] Marchand, F., and Ahmed, A. M., 1990, ''Investigation of the Laminate Structure of Lumbar Disc Annulus Fibrosus,'' Spine, **15**, No. 5, pp. 402–410.

[5] Cassidy, J. J., Hiltner, A., and Baer, E., 1989, ''Hierarchical Structure of the Intervertebral Disc,'' Connect. Tissue Res., **23**, pp. 75–88.

[6] Horton, W. G., 1958, ''Further Observations on the Elastic Mechanism of the Intervertebral Disc,'' J. Bone Jt. Surg., **40B**, No. 3, pp. 552–557.

[7] Hsu, E. W., and Setton, L. A., 1999, ''Diffusion Tensor Microscopy of the Intervertebral Disc Annulus Fibrosus,'' Magn. Reson. Med., **41**, No. 5, pp. 992–999.

[8] Acaroglu, E. R., Iatridis, J. C., Setton, L. A., Foster, R. J., Mow, V. C., and Weidenbaum, M., 1995, ''Degeneration and Aging Affect the Tensile Behavior of Human Lumbar Annulus Fibrosus,'' Spine, **20**, No. 24, pp. 2690–2701.

[9] Ebara, S., Iatridis, J. C., Setton, L. A., Foster, R. J., Mow, V. C., and Weidenbaum, M., 1996, ''Tensile Properties of Nondegenerate Human Lumbar Anulus Fibrosus,'' Spine, **21**, No. 4, pp. 452–461.

[10] Galante, J., 1967, ''Tensile Properties of the Human Lumbar Annulus Fibrosus,'' Acta Orthop. Scand. Suppl., **100**, pp. 1–91.

[11] Wu, H. C., and Yao, R. F., 1976, ''Mechanical Behavior of the Human Annulus Fibrosus,'' J. Biomech., **9**, pp. 1–7.

[12] Adams, M. A., and Green, T. P., 1993, ''Tensile Properties of the Annulus Fibrosus,'' Eur. Spine J., **2**, pp. 203–208.

[13] Kasra, M., Pranianpour, M., Wang, J. L., Shirazi-Adl, A., and Grynpas, M. D., 1997, ''Effect of Strain Rate on Failure Behavior of the Anulus Fibrosus in Tension,'' ASME Adv. Bioeng., **BED-36**, pp. 205–206.

[14] Fujita, Y., Duncan, N. A., and Lotz, J., 1997, ''Radial Tensile Properties of the Lumbar Anulus Fibrosus are Site and Degeneration Dependent,'' J. Orthop. Res., **15**, pp. 814–819.

[15] Marchand, F., and Ahmed, A. M., 1989, ''Mechanical Properties and Failure Mechanisms of the Lumbar Disc Annulus,'' Trans. Orthop. Res. Soc., **14**, p. 355.

[16] Nachemson, A., 1963, ''Influence of Spinal Movements on the Lumbar Intradiscal Pressure and on the Tensile Stresses in the Annulus Fibrosus,'' Acta Orthop. Scand., **33**, pp. 183–207.

[17] Stokes, I. A. F., 1987, ''Surface Strain on Human Intervertebral Discs,'' J. Orthop. Res., **5**, pp. 348–355.

[18] Goel, V. K., Kim, Y. E., Lim, T. H., and Weinstein, J. N., 1988, ''Analytical Investigation of the Mechanics of Spinal Instrumentation,'' Spine, **13**, No. 9, pp. 1003–1011.

[19] Goel, V. K., Monroe, B. T., Gilbertson, L. G., and Brinckmann, P., 1995, ''Interlaminar Shear Stresses and Laminae Separation in a Disc; Finite Element Analysis of the L3–L4 Motion Segment Subjected to Axial Compressive Loads,'' Spine, **20**, No. 6, pp. 689–698.

[20] Shirazi-Adl, S. A., Shrivastava, S. C., and Ahmed, A. M., 1984, ''Stress Analysis of the Lumbar Disc-Body Unit in Compression: a 3D Nonlinear Finite Element Study,'' Spine, **9**, No. 2, pp. 120–134.

[21] Shirazi-Adl, A., 1994, ''Nonlinear Stress Analysis of the Whole Lumbar Spine in Torsion—Mechanics of Facet Articulation,'' J. Biomech., **27**, No. 3, pp. 289–299.

[22] Ueno, K., and Liu, Y. K., 1987, ''Three-Dimensional Nonlinear Finite Element Model of Lumbar Intervertebral Joint in Tension,'' ASME J. Biomech. Eng., **109**, pp. 200–209.

[23] Natarajan, R. N., Ke, J. H., and Andersson, G. B. J., 1994, ''A Model to Study the Disc Degeneration Process,'' Spine, **19**, No. 3, pp. 259–265.

[24] Belytschko, T., Kulak, R. F., and Schultz, A. B., 1974, ''Finite Element Stress Analysis of an Intervertebral Disc,'' J. Biomech., **7**, pp. 277–285.

[25] Spilker, R. L., Jakobs, D. M., and Schultz, A. B., 1986, ''Material Constants for a Finite Element Model of the Intervertebral Disc With a Fiber Composite Annulus,'' ASME J. Biomech. Eng., **108**, pp. 1–11.

[26] Argoubi, M., and Shirazi-Adl, A., 1996, ''Poroelastic Creep Response Analysis of a Lumbar Motion Segment in Compression,'' J. Biomech., **29**, No. 10, pp. 1331–1339.

[27] Duncan, N. A., Ashford, F. A., and Lotz, J. C., 1996, ''The Effect of Strain Rate on the Axial Stress–Strain Response of the Human Annulus Fibrosus in Tension and Compression: Experiment and Poroelastic Finite Element Predictions,'' ASME Adv. Bioeng., **33**, pp. 401–402.

[28] Laible, J. P., Pflaster, D. S., Krag, M. H., Simon, B. R., and Haugh, L. D., 1993, ''Poroelastic-Swelling Finite Element Model With Application to the Intervertebral Disc,'' Spine, **18**, No. 5, pp. 659–670.

[29] Simon, B. R., Wu, J. S. S., Carlton, M. W., Evans, J. H., and Kazarian, L. E., 1985, ''Structural Models for Human Spinal Motion Segments Based on a Poroelastic View of the Intervertebral Disc,'' ASME J. Biomech. Eng., **107**, pp. 327–335.

[30] Spencer, A. J. M., 1972, *Deformations of Fibre-Reinforced Materials*, Oxford University Press.

[31] Spencer, A. J. M., 1984, ''Constitutive Theory for Strongly Anisotropic Solids,'' in: *Continuum Theory of the Mechanics of Fibre-Reinforced Composites*, A. J. M. Spencer, ed., Springer-Verlag, pp. 1–32.

[32] Best, B. A., Guilak, F., Setton, L. A., Zhu, W., Saed-Nejad, F., Ratcliffe, A., Weidenbaum, M., and Mow, V. C., 1994, ''Compressive Mechanical Properties of the Human Annulus Fibrosus and Their Relationship to Biochemical Composition,'' Spine, **19**, No. 2, pp. 212–221.

[33] Spencer, A. J. M., 1971, ''Theory of Invariants,'' in: *Continuum Physics*, A. C. Eringen, ed., Academic Press, pp. 239–353.

[34] Ting, T. C. T., 1996, *Anisotropic Elasticity*, Oxford University Press.

[35] Fujita, Y., Duncan, N. A., and Lotz, J. C., 1996, ''Anisotropic Shear Behavior of the Annulus Fibrosus: Effect of Harvest Site and Tissue Prestrain,'' Trans. Orthop. Res. Soc., **21**, p. 271.

[36] Iatridis, J. C., Kumar, S., Krishnan, L., Rawlins, B. A., Weidenbaum, M., and Mow, V. C., 1996, ''Shear Mechanical Behavior of the Human Lumbar Annulus Fibrosus and the Effects of Degeneration,'' ASME Adv. Bioeng., **BED-33**, pp. 149–150.

[37] Skaggs, D. L., Weidenbaum, M., Iatridis, J. C., Ratcliffe, A., and Mow, V. C., 1994, ''Regional Variation in Tensile Properties and Biochemical Composi-

tion of the Human Lumbar Annulus Fibrosus,'' Spine, **19**, No. 12, pp. 1310–1319.
[38] Bovendeerd, P. H. M., Arts, T., Huyghe, J. M., Van Campen, D. H., and Reneman, R. S., 1992, ''Dependence of Local Left Ventricular Wall Mechanics on Myocardial Fiber Orientation: a Model Study,'' J. Biomech., **25**, No. 10, pp. 1129–1140.
[39] Guccione, J. M., McCulloch, A. D., and Waldman, L. K., 1991, ''Passive Material Properties of Intact Ventricular Myocardium Determined From a Cylindrical Model,'' ASME J. Biomech. Eng., **113**, pp. 42–55.
[40] Humphrey, J. D., and Yin, F. C. P., 1987, ''New Constitutive Formulation for Characterizing the Mechanical Behavior of Soft Tissues,'' Biophys. J., **52**, pp. 563–570.
[41] Humphrey, J. D., Strumpf, R. K., and Yin, F. C. P., 1990, ''Determination of a Constitutive Relation for Passive Myocardium: I. A New Functional Form,'' ASME J. Biomech. Eng., **112**, pp. 333–339.
[42] Taber, L. A., 1991, ''On a Nonlinear Theory for Muscle Shells: Part II—Application to the Beating Left Ventricle,'' ASME J. Biomech. Eng., **113**, pp. 63–71.
[43] Puso, M. A., and Weiss, J. A., 1998, ''Finite Element Implementation of Anisotropic Quasi-Linear Viscoelasticity Using a Discrete Spectrum Approximation,'' ASME J. Biomech. Eng., **120**, pp. 62–70.
[44] Drost, M. R., Willems, P., Snijders, H., Huyghe, J. M., Janssen, J. D., and Huson, A., 1995, ''Confined Compression of Canine Annulus Fibrosus Under Chemical and Mechanical Loading,'' ASME J. Biomech. Eng., **117**, pp. 390–396.
[45] Iatridis, J. C., Setton, L. A., Foster, R. J., Rawlins, B. A., Weidenbaum, M., and Mow, V. C., 1998, ''Degeneration Affects the Anisotropic and Nonlinear Behaviors of Human Annulus Fibrosus in Compression,'' J. Biomech., **31**, pp. 535–544.
[46] Gu, W. Y., Mao, X. G., Foster, R. J., Weidenbaum, M., Mow, V. C., and Rawlins, B. A., 1999, ''The Anisotropic Hydraulic Permeability of Human Lumbar Anulus Fibrosus, Influence of Age, Degeneration, Direction, and Water Content,'' Spine, **24**, pp. 2449–2455.
[47] Seroussi, R. E., Krag, M. H., Muller, D. L., and Pope, M. H., 1989, ''Internal Deformations of Intact and Denucleated Human Lumbar Discs Subjected to Compression, Flexion, and Extension Loads,'' J. Orthop. Res., **7**, pp. 122–131.